ADVANCED FUNCTIONAL MATERIALS
www.afm-journal.de
www.MaterialsViews.com

3D Micromolding of Arrayed Waveguide Gratings on Upconversion Luminescent Layers for Flexible Transparent Displays without Mirrors, Electrodes, and Electric Circuits

Satoshi Watanabe, Takeo Asanuma, Takafumi Sasahara, Hiroshi Hyodo, Mutsuyoshi Matsumoto, and Kohei Soga**

A new technique for the fabrication of arrayed waveguide gratings on upconversion luminescent layers for flexible transparent displays is reported. Ho^{3+}- and Yb^{3+}-codoped $NaYF_4$ nanoparticles are synthesized by hydrothermal techniques. Transparent films consisting of two transparent polymers on the $NaYF_4$ nanoparticle films exhibit mechanical flexibility and high transparence in visible region. Patterned $NaYF_4$ nanoparticle films are fabricated by calcination-free micromolding in capillaries. Arrayed waveguide gratings consisting of the two transparent polymers are formed on the patterned $NaYF_4$ nanoparticle films by micromolding in capillaries. Green and red luminescence is observed from the upconversion luminescent layers of the $NaYF_4$ nanoparticle films in the arrayed waveguide gratings under excitation at 980 nm laser light. Arrayed waveguide gratings on the upconversion luminescent layers are fabricated with Er^{3+}-doped $NaYF_4$ nanoparticles which can convert two photons at 850 and 1500 nm into single photon at 550 nm. These results demonstrate that flexible transparent displays can be fabricated by constructing arrayed waveguide gratings on upconversion luminescent layers, which can operate in nonprojection mode without mirrors, transparent electrodes, and electric circuits.

1. Introduction

The fabrication of organic semiconductor devices on flexible plastic sheets has attracted much attention for organic thin film solar cells,[1] field-effect transistors,[2] and light-emitting diodes[3] because of their unique advantages such as its light weight, flexibility, and low cost. Organic light-emitting displays consisting of a cathode, electron-transport layer, organic luminescent layer, hole-transport layer, and an anode have already been used in large-size displays and mobile displays. These organic light-emitting displays are operated in the active matrix mode using arrayed electrodes and organic field-effect transistors.

Photoluminescence displays enable the fabrication of flexible transparent displays with high transparency without transparent electrodes and electric circuits.[4] In addition, photoluminescence devices also attract much attention for head-up displays, projecting meter information such as speed, position, and direction on the large-scale front glasses of airplanes and ships, which require high transparency, large-scale fabrication, and long-operating lifetime. Photon upconversion luminescent (UCL) materials, which can convert infrared light into visible light, helps in solving the low-resolution problems of photoluminescent transparent displays.[5] 3D images can be projected in the UCL displays projected with near-infrared light in an transparent polymer matrix dispersed with rare-earth-ion-doped nanoparticles. However, these projection type displays have potential problems in device size because of the necessity of Garvano mirrors and condensers.

To solve these problems, we have considered the fabrication of arrayed waveguide gratings[6] (AWGs) consisting of waveguides (core) of transparent polymers surrounded by a clad matrix on patterned UCL layers (**Figure 1**). AWG-UCL devices allow for the fabrication of transparent upconversion displays operated in nonprojection mode by the excitation of patterned UCL layers on the cross-point of the waveguides with two near-infrared lights at 850 and 1500 nm through *X*-axis and *Y*-axis waveguides. To fabricate AWG-UCL devices, the fabrication technique of UCL layers on transparent polymer films is required.

Rare-earth-ion-doped phosphor materials have attracted much attention for photoluminescent crystals,[7] bioimaging,[8] and organic solar cells used as light condensing layers in the near-infrared region.[9] Rare-earth-ion-doped phosphor films

Dr. S. Watanabe
Applied Chemistry and Biochemistry
Graduate School of Science and Technology
Kumamoto University
2-39-1 Kurokami, Kumamoto 860-8555, Japan
E-mail: watasato@kumamoto-u.ac.jp
T. Asanuma, T. Sasahara, Prof. M. Matsumoto, Prof. K. Soga
Department of Materials Science and Technology
Tokyo University of Science
6-3-1 Niijuku, Katsushika-ku, Tokyo 125-8585, Japan
E-mail: mail@ksoga.com
Dr. H. Hyodo
Institute of Multidisciplinary Research for Advanced Materials
Tohoku University
Katahira 2-1-1, Aoba-ku, Sendai 980-8577, Japan

DOI: 10.1002/adfm.201500542

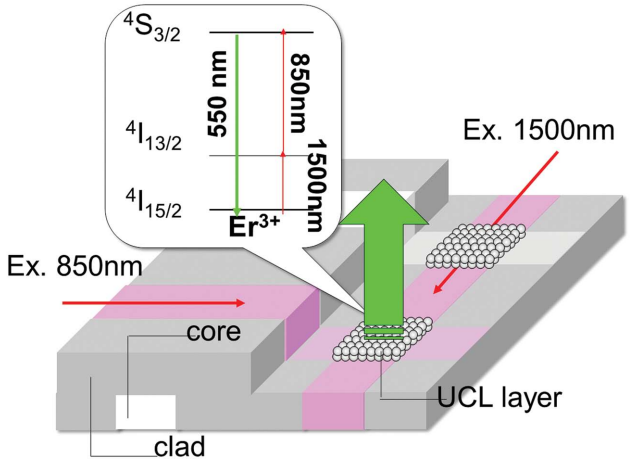

Figure 1. Illustration of AWG-UCL devices for the fabrication of flexible transparent displays without a mirror, transparent electrode, or transistor circuits.

have been fabricated on solid substrates using electrophoresis,[10] screen printing,[11] sol–gel techniques,[12] and self-assembly.[13] These techniques are based on the patterning of precursor films of UCL layers on solid substrates using photolithography and soft lithography. However, a calcination process is required after the formation of the precursor films on solid substrates, rendering the fabrication of UCL layers on low thermal resistance films of polymer sheets difficult. We have reported calcination-free lithography for the fabrication of UCL layers on flexible plastic sheets using rare-earth-ion-doped nanoparticles, which requires no calcination process after the formation of rare-earth-ion-doped nanoparticle films. We successfully obtained patterned UCL layers on flexible plastic sheets using calcination-free techniques in photolithography,[14] micromolding in capillaries which is a type of soft lithography,[15] and self-assembly.[16]

In this study, we fabricate arrayed waveguide gratings consisting of two types of transparent polymers on patterned UCL layers of rare-earth-ion-doped nanoparticle films. We synthesize rare-earth-ion-doped nanoparticles, which can be excited with laser beams at 980 or 850 and 1500 nm. We used micromolding in capillaries for the patterning of transparent polymer films and rare-earth-ion-doped nanoparticle films to fabricate AWGs and patterned UCL layers, respectively. The samples were analyzed using fluorescent spectroscopy, ultraviolet–visible spectroscopy, optical microscopy, laser microscopy, scanning electron microscopy (SEM), and energy dispersive X-ray (EDX) spectroscopy.

2. Results and Discussion

Visible UCL and near-infrared fluorescence of the Ho^{3+}-doped $NaYF_4$ nanoparticles were measured under excitation light at 980 nm. **Figure 2**a,b presents visible UCL and near-infrared fluorescent spectra of the Ho^{3+}-doped $NaYF_4$ nanoparticles. UCL appeared at 540, 650, and 760 nm attributed to transitions of $^5F_4$-$^5I_8$, $^5F_5$-$^5I_8$, and $^5F_5$-$^5I_7$ of Ho^{3+}, respectively. Fluorescence was only emitted at 1200 nm assigned to $^5I_7$-$^5I_8$ transition of Ho^{3+}. The absence of fluorescence at 1000 nm attributed to the $^2F_{5/2}$-$^2F_{7/2}$ transition of Yb^{3+} indicates dominance of the energy transfer from the $^2F_{5/2}$ state of Yb^{3+} to the $^5I_6$ state of Er^{3+}.

The patterned Ho^{3+}-doped $NaYF_4$ nanoparticle films were fabricated by immersing Ho^{3+}-doped $NaYF_4$ nanoparticle films on the photoresist films patterned with micromolding in capillaries into acetone for the liftoff process. **Figure 3**a presents an optical microscope image of the photoresist films patterned by micromolding in capillaries. Holes at a diameter of 50 μm were formed in the photoresist films. The surfaces of the glass plates were exposed in the hole regions surrounded by the photoresist films. Figure 3b presents an optical microscope image of the Ho^{3+}-doped $NaYF_4$ nanoparticle films fabricated on the entire area of the patterned photoresist films using cast techniques. Ho^{3+}-doped $NaYF_4$ nanoparticle films were formed both on the surface of the glass plates in the hole regions and the photoresist films. Figure 3c presents an optical microscope image of the Ho^{3+}-doped $NaYF_4$ nanoparticle films after dissolving the photoresist films with acetone. The liftoff process leaves the Ho^{3+}-doped $NaYF_4$ nanoparticle films only on the surface of the glass plates in the hole regions. Figure 3d presents an SEM image of the Ho^{3+}-doped $NaYF_4$ nanoparticle films after the liftoff. The Ho^{3+}-doped $NaYF_4$ nanoparticle films consist of Ho^{3+}-doped $NaYF_4$ nanoparticles with a diameter of 100 nm. These results demonstrate that the patterned Ho^{3+}-doped $NaYF_4$ nanoparticle films can be fabricated by micromolding in capillaries, casting, and liftoff processes.

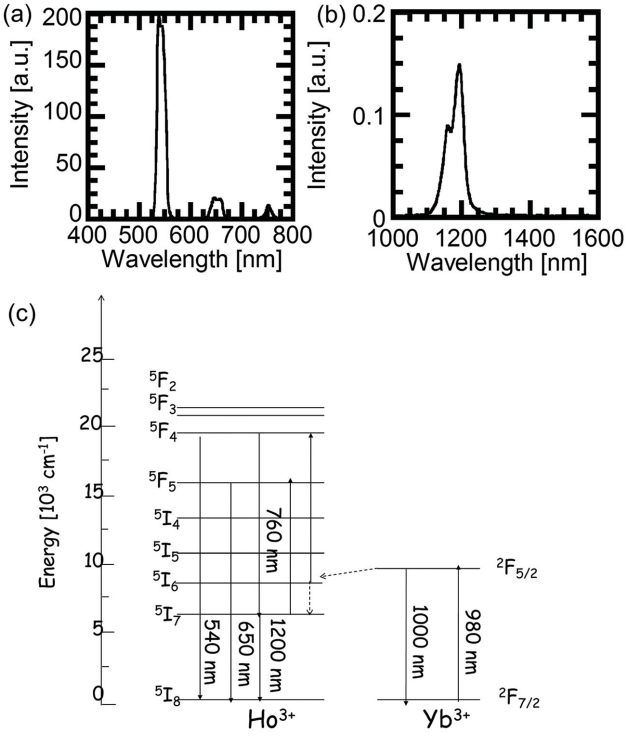

Figure 2. a) UCL and b) near-IR fluorescent spectra of Ho^{3+}-doped $NaYF_4$ nanoparticles excited with 980 nm laser beams. c) Energy diagram of UCL and near-IR fluorescence from Ho^{3+} and Yb^{3+} in low-phonon vibration materials.[17]

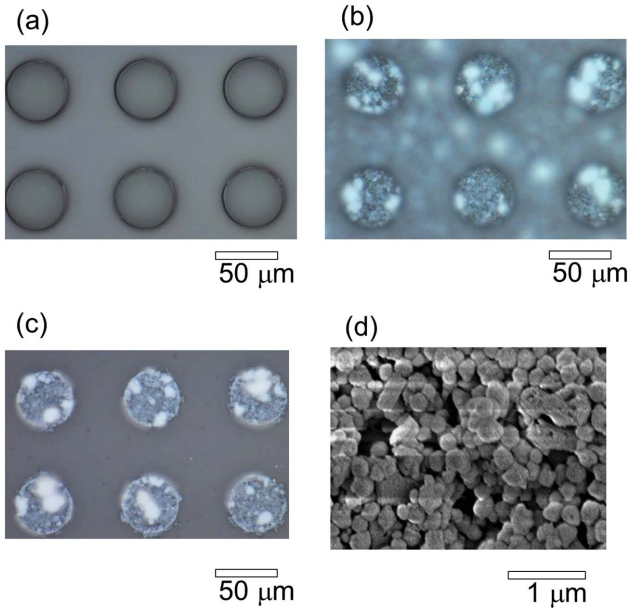

Figure 3. Optical microscope images of a) patterned photoresist films, b) Ho^{3+}-doped $NaYF_4$ nanoparticle films on the entire area of the patterned photoresist films, c) patterned Ho^{3+}-doped $NaYF_4$ nanoparticle films. d) SEM image of Ho^{3+}-doped $NaYF_4$ nanoparticle films (also shown in Figure 9a).

We fabricate Ho^{3+}-doped $NaYF_4$ nanoparticle films with variations in the fabrication conditions. **Figure 4** presents laser microscope images of the Ho^{3+}-doped $NaYF_4$ nanoparticle films with variations in the particle size, concentration of the dispersion, and volume ratio of EtOH and water. The thickness of the Ho^{3+}-doped $NaYF_4$ nanoparticle films is 1–2 μm. Decreases in the particle size and concentration and an increase in the volume ratio lead to a tendency of the formation of flat films of Ho^{3+}-doped $NaYF_4$ nanoparticles. We investigated the precise control of the film thickness of the Ho^{3+}-doped $NaYF_4$ nanoparticle films fabricated by casting and performed quantitative analysis of the surface roughness using atomic force microscopy. These results demonstrate the formation of flat films of Ho^{3+}-doped $NaYF_4$ nanoparticles with variations in the fabrication conditions.

We performed ultraviolet–visible absorption and phase-shifting laser microscope observations of the stacked films of ethoxylated bisphenol A diacrylate (EBPADA), polydimethyl siloxane (PDMS), and Ho^{3+}-doped $NaYF_4$ nanoparticles as core, clad, and UCL layers, respectively. **Figure 5**a,b shows visual observation and transmittance spectrum of Ho^{3+}-doped $NaYF_4$ nanoparticle films fabricated between 10 μm EBPADA layers covered with several mm PDMS films. As observed in Figure 5a, the stacked films consisting of core, clad, and UCL materials exhibit mechanical flexibility. The transparency of the stacked films is higher than that of the Ho^{3+}-doped $NaYF_4$ nanoparticle films owing to a decrease in the Mie scatterings near the ultraviolet regions. Thus, the refractive index of EBPADA was adjusted to that of the Ho^{3+}-doped $NaYF_4$ nanoparticles. Figure 5c–e presents the interference pattern image, phase shift distribution image, and profile of the arrayed waveguides fabricated with EBPADA and PDMS. As observed in Figure 5c, two types of interference patterns were distributed in the period of 50 μm width. This image was converted into phase distribution images, as observed in Figure 5d. The phase shift distribution is proportional to a difference of refractive index as demonstrated in the following equation[18]

$$\Psi(x,y) = 2\pi t \frac{n_2(x,y) - n_1}{\lambda_0} \quad (1)$$

where $\Psi(x,y)$ is the phase distribution, t is the thickness of the layers, λ_0 is the wavelength of the laser beam, and n_1 and $n_2(x,y)$ are the refractive index of the clad and core, respectively. The phase shift distribution of the refractive index difference of EBPADA and PDMS was examined, and the bright and dark region represented the EBPADA core and PDMS clad, respectively. Δn ($=n_2 - n_1$) is equal to 0.04, 0.10, 0.16, which is calculated with the above profile of the phase shift image. n_2 and n_1 are also estimated to be ≈1.50 and ≈1.40 using Abbe's refractometer, leading to $\Delta n = 0.10$. We are now attempting to estimate the local refractive index of the arrayed waveguides

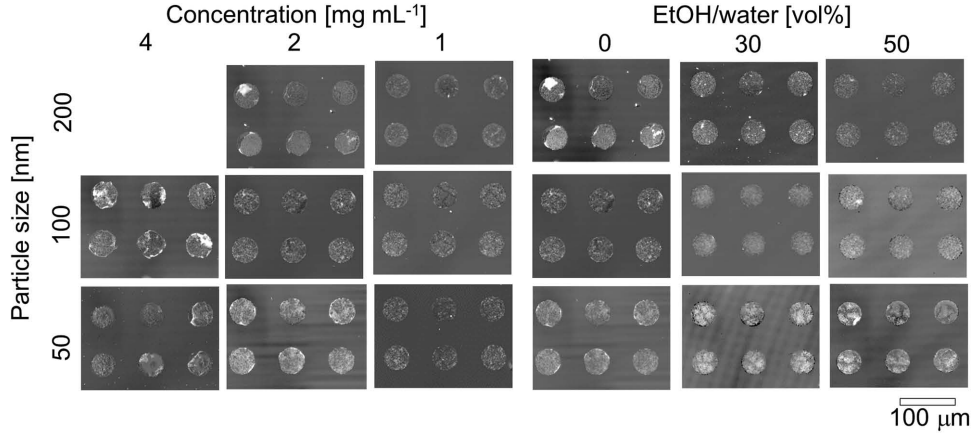

Figure 4. Laser microscope images of patterned Ho^{3+}-doped nanoparticle films fabricated with variations in the particle size of Ho^{3+}-doped nanoparticles, a concentration of Ho^{3+}-doped nanoparticle dispersion, and a volume ratio of water and EtOH in Ho^{3+}-doped nanoparticle dispersion.

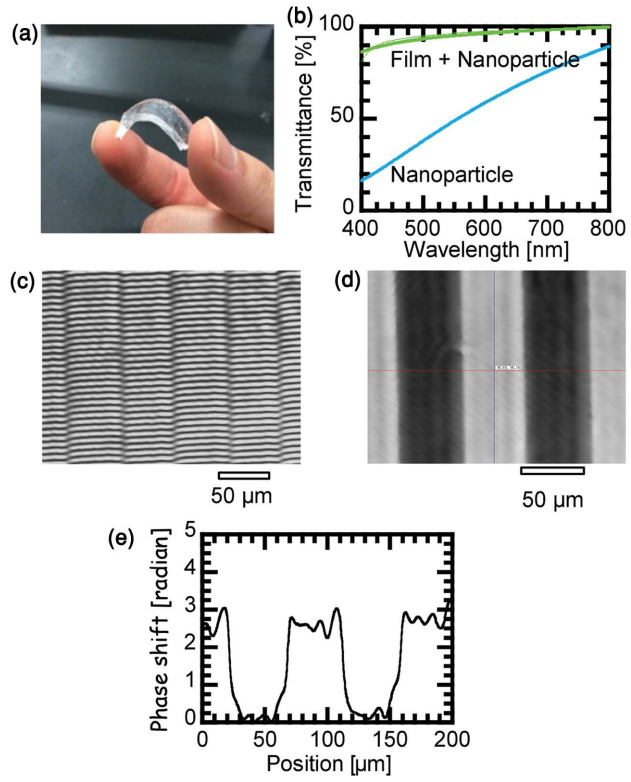

Figure 5. a) Photograph of PDMS/EBPADA/Ho^{3+}-doped nanoparticles/EBPADA/PDMS-stacked samples, b) transmittance spectra of the stacked sample and Ho^{3+}-doped nanoparticle films on glass plates, c) interference pattern image at 630 nm, d) phase-shift image, and e) profile of EBPADA waveguides surrounded by PDMS molds. Cast films of Ho^{3+}-doped nanoparticles were formed on 2 mm thickness PDMS, and then spin-coated films (thickness: 50 μm) of EBPADA were fabricated on the cast films. Finally, PDMS films (thickness: 2 mm) were formed on the spin-coated films.

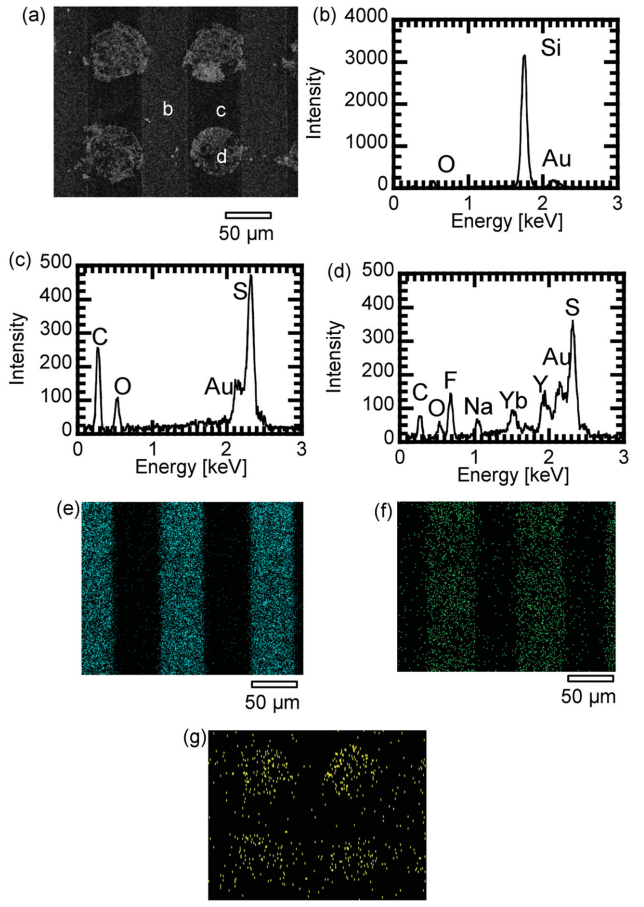

Figure 6. a) SEM image, EDX spectra at points (b–d), and EDX mapping of e) Si, f) S, and g) F in Ho^{3+}-doped $NaYF_4$ nanoparticle films fabricated on arrayed waveguides surrounded by PDMS molds (also shown in Figure 9d).

by studying the phase shift related to the film thickness and tuning the experimental conditions of the laser interference microscope observations. These results demonstrate the high transparency of the PDMS/EBPADA/Ho^{3+}-doped $NaYF_4$ nanoparticle films in the visible region and phase shift distribution based on the refractive index in the arrayed waveguides fabricated with the EBPADA waveguides surrounded by the PDMS clads.

We fabricated the EBPADA waveguides surrounded by the PDMS clads on the Ho^{3+}-doped $NaYF_4$ nanoparticle films by micromolding in capillaries to fabricate the arrayed waveguides on the UCL layers. **Figure 6**a presents an SEM image of the arrayed waveguides surrounded by the PDMS molds on the Ho^{3+}-doped $NaYF_4$ nanoparticle films. The disk films at a diameter of 50 μm consisting of the Ho^{3+}-doped $NaYF_4$ nanoparticle films on the arrayed waveguides were observed. Figure 6b–d shows EDX spectra on the Ho^{3+}-doped $NaYF_4$ nanoparticle films, arrayed waveguides, and PDMS molds in the SEM images. Characteristic X-rays of silicon and oxygen attributed to PDMS, carbon, oxygen, and sulfur assigned to EBPADA, and fluorine, sodium, ytterbium, and yttrium attributed to the Ho^{3+}-doped $NaYF_4$ nanoparticles are observed in Figure 6b–d, respectively. The gold signals are assigned to the sputtered films covering the samples for the SEM observations. Figure 6e–g shows elemental mapping of silicon, sulfur, and fluorine on the arrayed waveguides surrounded by the PDMS molds on the Ho^{3+}-doped $NaYF_4$ nanoparticle films. Fluorine, sulfur, and silicon are distributed in the Ho^{3+}-doped $NaYF_4$ nanoparticle films, arrayed waveguides, and PDMS molds, respectively. These results indicate that the EBPADA waveguides surrounded by the PDMS molds were formed on the patterned Ho^{3+}-doped $NaYF_4$ nanoparticle films. In addition, the Ho^{3+}-doped $NaYF_4$ nanoparticle films were immobilized on the EBPADA waveguides due to the polymerization, which leads to an increase in the mechanical stability of the UCL layers on the substrates.

We fabricated the second layer of the arrayed waveguides on the above samples to construct AWG-UCL devices. **Figure 7**a presents an optical microscope image of the AWG-UCL devices. The arrayed waveguides were formed on the UCL layers across the first layer of the arrayed waveguides. Figure 7b,c shows UCL images of the AWG-UCL devices excited with 980 nm laser light. Green and red UCL were observed from the Ho^{3+}-doped $NaYF_4$ nanoparticle films in the AWG-UCL devices.

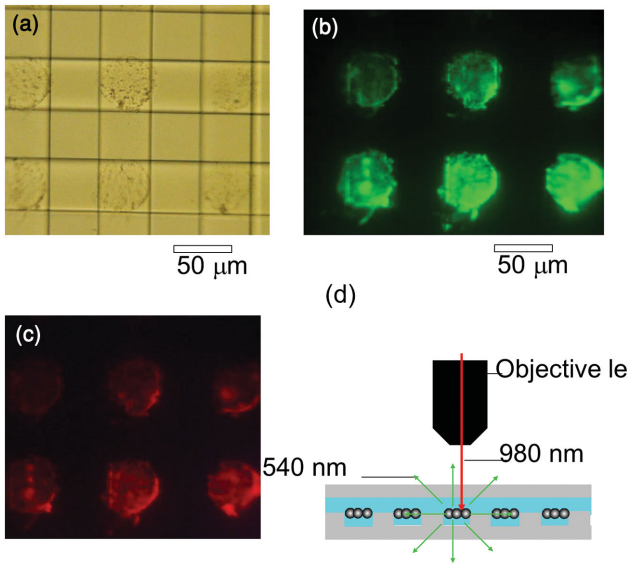

Figure 7. a) Optical microscope and UCL images at b) 550 and c) 650 nm of AWGs on the patterned Ho^{3+}-doped $NaYF_4$ nanoparticle films excited at 980 nm (also shown in Figure 9f). d) Illustration of cross-sectional view of AWG-UCL devices in UCL observation using near-infrared beams irradiated through an objective lens.

These results demonstrate that the AWG-UCL devices can be fabricated by constructing the AWGs on the patterned UCL layers.

We fabricated the AWGs on the patterned UCL layers, which can be excited with light at 850 and 1500 nm by synthesizing Er^{3+}-doped $NaYF_4$ nanoparticles. **Figure 8**a,b presents UCL and fluorescent spectra of the Er^{3+}-doped $NaYF_4$ nanoparticles fabricated with variation in the concentration of Er^{3+}. An increase in the concentration of Er^{3+} causes a decrease in the UCL at 545 nm attributed to the $^2H_{11/2}$–$^4I_{15/2}$ transition and an increase in the UCL at 645 nm assigned to the $^4F_{9/2}$–$^4I_{15/2}$ transition. The intensity ratio of the fluorescence at 990 nm attributed to the $^4I_{11/2}$–$^4I_{15/2}$ transition and that at 1500 nm assigned to the $^4I_{13/2}$–$^4I_{15/2}$ transition remain unchanged by varying the concentration of Er^{3+}. Figure 8c presents an energy band diagram of Er^{3+} for explanation of the UCL and fluorescence mechanism.[13] Figure 8d,e presents optical microscope and UCL images of the AWGs on the patterned Er^{3+}-doped $NaYF_4$ nanoparticle films. The AWGs were formed on the Er^{3+}-doped $NaYF_4$ nanoparticle films. The UCL appears on the Er^{3+}-doped $NaYF_4$ nanoparticle films excited with 850 nm (irradiated from the bottom side in the image) and 1500 nm laser light (irradiated from the left side in the image) through the second and first waveguides, respectively. These results demonstrate that the AWG-UCL devices excited with two wavelength light can be fabricated.

3. Conclusion

We discuss new AWG-UCL devices fabricated with calcination-free micromolding in capillaries. Er^{3+}- or Ho^{3+}-doped $NaYF_4$ nanoparticles were synthesized using hydrothermal techniques. AWGs consisting of flexible high and low refractive

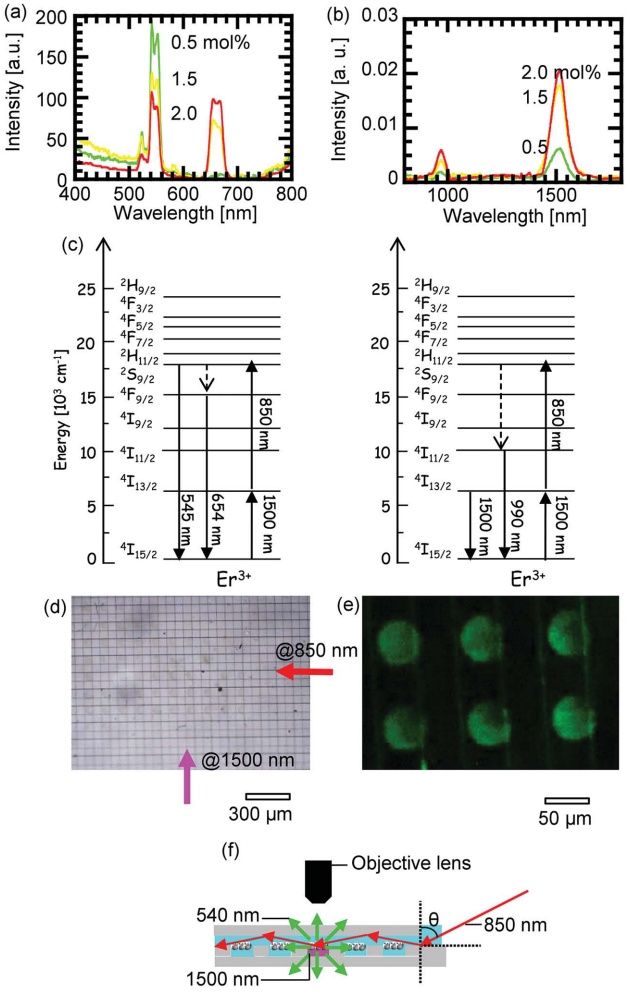

Figure 8. a) UCL and b) near-IR fluorescent spectra of $NaYF_4$ nanoparticles doped with Er^{3+} at a molar ratio of 0.5%, 1.5%, and 2.0%, excited with two laser beams at 850 and 1500 nm. c) Energy diagrams of UCL and near-IR fluorescence from Er^{3+} in $NaYF_4$ matrix excited with two laser lights at 850 and 1500 nm. d) Optical microscope, e) UCL images and illustration of cross-sectional view of patterned Er^{3+}-doped $NaYF_4$ nanoparticle films in AWGs excited with two laser beams at 850 and 1500 nm through the waveguides. The laser beams at 850 and 1500 nm were irradiated at the open ends of AWGs at an incident angle of 60°.

index polymers were formed on the patterned $NaYF_4$ nanoparticle films. The AWG-UCL devices were characterized using optical microscopy, SEM, and laser microscopy. The AWG-UCL devices can serve as upconversion displays without projection instruments.

AWG-UCL devices can drive UCL transparent displays with projection instrument-free systems, which is based on a new type of passive matrix type displays. This technology enables imaging on transparent displays fabricated without mirrors, transparent electrodes, and transistor circuits. The UCL layers were fabricated with rare-earth-ion-doped phosphor films, leading to long-operating lifetime compared with organic light-emitting materials. In the future, nanopatterning of the AWGs and UCL layers will enable the application of AWG-UCL devices to high-transparence displays. In other approaches, the patterning of functional

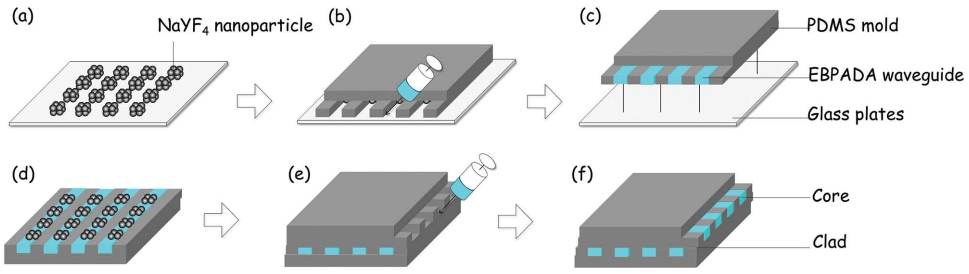

Figure 9. Fabrication scheme: a) patterning of $NaYF_4$ nanoparticle film on hydrophobic glass plates, b) injection and polymerization of the first layer of the arrayed waveguides, c,d) peeling off of the arrayed waveguides on the UCL layer, e) injection and polymerization of second layer of arrayed waveguides, and f) formation of AWGs on UCL layers.

ceramic nanoparticles that serve as sensors or memories on the AWGs will lead to the creation of next-generation photonic devices such as phototransistors and high-density memories.

4. Experimental Section

Materials: $Y(NO_3)_3$ (Kanto Chemical), $Yb(NO_3)_3$ (Sigma-Aldrich), $Ho(NO_3)_3$ (Sigma-Aldrich), $Er(NO_3)_3$ (Sigma-Aldrich), and NaF (Kanto Chemical) were used for the synthesis of $NaYF_4$ nanoparticles. EBPADA as a high refractive index polymer, pentaerythritol tetrakis-3-mercaptopropionate (PEMP) for adjusting the refractive index of the EBPADA films, and benzophenone as a polymeric initiator were purchased from Hitachi Chemical Co., Ltd., Sakai Chemical Industry Co., Ltd., and Sigma-Aldrich, respectively. Calcium chloride was obtained from Wako. Glass plates and Si molds were obtained from Matsunami Glass Ind., Ltd. and Kyodo International Inc., respectively. The hexamethyldisilazane used for the modification of the glass plates to hydrophobic surfaces was purchased from Sigma-Aldrich. PDMS precursor (PDMS SILPOT 184 W/C) and its polymeric initiator (SILPOT 184 W/C curing agent) used for the fabrication of PDMS molds were purchased from Dow Corning Toray. Az 1500 of photoresist was obtained from AZ Electronic Materials. Acetone and chloroform used for cleaning the substrates were purchased from Wako.

Synthesis of $NaYF_4$ Nanoparticles for Excitation at 980 nm:[19] First, 5.55 mmol $Y(NO_3)_3$, 1.50 mmol $Ho(NO_3)_3$, and 0.45 mmol $Yb(NO_3)_3$ were dissolved in 20 mL of pure water [Y:Ho:Yb = 74:20:6 (mol%)]. Then, 30 mmol NaF was dissolved in 30 mL of pure water at a water temperature of 75 °C. The two solutions were mixed and stirred for 1 h at 75 °C. The precipitates were washed centrifugally with pure water three times (15 000 G, 10 min) and dried in a desiccator at 80 °C overnight. The white powder was pounded in a mortar and was heated in air at 400 °C for 1 h (at a rate of 20 °C min^{-1}). HF gas was trapped in the water dissolved with 60 mmol $CaCl_2$.

Synthesis of $NaYF_4$ Nanoparticles for Excitation at 850 and 1500 nm:[19] $Y(NO_3)_3$ and $Er(NO_3)_3$ were dissolved in 20 mL of pure water [Y:Er (total 7.5 mmol) = 99.5:0.5, 99.0:1.0, or 98.0:2.0 (mol%)]. Then, 30 mmol NaF was dissolved in 30 mL pure water at a temperature of 75 °C. The two solutions were mixed and stirred for 1 h at 75 °C. The precipitates were washed centrifugally with pure water three times (15 000 G, 10 min) and dried in a desiccator at 80 °C overnight. The white powder was pounded in a mortar and was heated in air atmosphere at 400 °C for 5 h (at a rate of 20 °C min^{-1}). HF gas was trapped in the water dissolved with 60 mmol $CaCl_2$.

Preparation of Hydrophobic Substrates and PDMS Molds: Glass plates were ultrasonicated in acetone and chloroform for 15 min each, exposed to UV/ozone atmosphere for 15 min, and then immersed in neat liquid of hexamethyldisilazane for 6 h. After a heat treatment at 110 °C for 30 min, self-assembled monolayers were formed on the glass plates. Liquid of SILPOT 184 and SILPOT 184 curing agent was mixed at a mixing ratio of 10:1 [wt%] and was then placed in a vacuum desiccator for 15 min to remove air bubbles. The mixture was poured on Si molds and then heated at 110 °C for 1 h.

Fabrication of AWGs on Patterned UCL Layers: The pillar type PDMS molds (diameter: 50 μm, pitch: 100 μm, depth: 10 μm) exposed to UV/ozone atmosphere were placed on the hydrophobic glass plates. A small droplet of Az 1500 photoresist solution diluted with ethanol at a half volume percent was placed at the open end of the PDMS molds. The photoresist solution was filled spontaneously into the channels by capillary force. Patterned photoresist films were formed on the hydrophobic glass plates. 100 μL of the $NaYF_4$ nanoparticle dispersion at the desired concentrations was cast on the patterned photoresist films followed by immersion in acetone for liftoff, resulting in the formation of patterned $NaYF_4$ nanoparticle films (**Figure 9**a). The line/space type PDMS molds were placed on the patterned $NaYF_4$ nanoparticle films. The position of the channels was adjusted on the patterned $NaYF_4$ nanoparticle films. A small droplet of a mixture of EBPADA and PEMP was placed at the open end of the line/space type PDMS molds (Figure 9b). After spontaneous filling and drying, UV light was irradiated on the entire area of the samples for polymerization, resulting in the formation of arrayed waveguides in the PDMS molds. The arrayed waveguides with the PDMS molds were peeled from the hydrophobic glass plates (Figure 9c,d). The line/space type PDMS molds were crossed on the arrayed waveguides, and the channels were placed on the patterned $NaYF_4$ nanoparticle films (Figure 9e). A small droplet of the mixture of EBPADA and PEMP was placed at the open end of the line/space type PDMS molds, and UV light was irradiated for polymerization, leading to the formation of AWGs (Figure 9f).

Characterization: Optical microscopic observations were performed with a BX-60 optical microscope (Olympus, Japan). Visible upconversion luminescent and near-IR fluorescent spectra were acquired using an RF-5000 visible spectrometer (Shimadzu, Japan) and a near-IR spectrometer (AvaSpec, USA) and semiconductor laser diodes (beam spot: 0.1–1 mm) operating at 850, 980, and 1500 nm, respectively. Visible UCL and near-IR fluorescence microscopic observations were performed with an IX-71 optical microscope (Olympus, Japan) using a band-pass filter at 550 or 650 nm and a short-pass filter at 800 nm. SEM observations were performed with an S-4200 microscope (Hitachi, Japan). The refractive index of arrayed waveguides was analyzed with a phase-shifting laser microscope equipped with a He–Ne laser at 632.8 nm (FK Opt Lab Co., Ltd.).

Acknowledgements

The authors thank the KEYENCE Corporation for the laser microscope used to analyze the thickness of the $NaYF_4$ nanoparticle films. This study was partly supported by JSPS KAKENHI (Grant No. 24750185) and The Kao Foundation for Arts and Sciences.

Received: February 8, 2015
Revised: April 25, 2015
Published online: June 5, 2015

[1] a) G. Yu, J. Gao, J. C. Hummelen, F. Wudl, A. J. Heeger, *Science* **1995**, *270*, 1789; b) W. Ma, C. Yang, X. Gong, K. Lee, A. J. Heeger, *Adv. Funct. Mater.* **2005**, *15*, 1617; c) G. Li, V. Shrotriya, J. Hung, Y. Yao, T. Moriarty, K. Emery, Y. Yang, *Nat. Mater.* **2005**, *4*, 864.

[2] a) J. C. Ribierre, T. Fujihara, S. Watanabe, M. Matsumoto, T. Muto, A. Nakao, T. Aoyama, *Adv. Mater.* **2010**, *22*, 1; b) J. C. Ribierre, S. Watanabe, M. Matsumoto, T. Muto, A. Nakao, T. Aoyama, *Adv. Mater.* **2010**, *22*, 4044; c) T. Minari, C. Liu, M. Kano, K. Tsukagoshi, *Adv. Mater.* **2012**, *24*, 299; d) R. H. Kim, H. J. Kim, I. Bae, S. K. Hwang, D. B. Velusamy, S. M. Cho, K. Takaishi, T. Muto, D. Hashizume, M. Uchiyama, P. André, F. Mathevet, B. Heinrich, T. Aoyama, D. E. Kim, H. Lee, J. C. Ribierre, C. Park, *Nat. Commun.* **2014**, *5*, 3583.

[3] a) L. S. Hung, C. W. Tang, M. G. Mason, *Appl. Phys. Lett.* **1997**, *70*, 152; b) J. Shi, C. W. Tang, *Appl. Phys. Lett.* **2002**, *80*, 3201; c) A. L. Briseno, S. C. B. Mannsfeld, M. M. Ling, S. Liu, R. J. Tseng, C. Reese, M. E. Roberts, Y. Yang, F. Wudl, Z. Bao, *Nature* **2006**, *444*, 913; d) J. H. Kim, M. Inoue, L. Zhao, T. Komino, S. Seo, J. C. Ribierre, C. Adachi, *Appl. Phys. Lett.* **2015**, *106*, 053302.

[4] a) C. Weder, C. Sarwa, A. Montali, C. Bastiaansen, P. Smith, *Science* **1998**, *279*, 835; b) D. Choi, K. Choi, B. Byun, S. Yi, *IEEE Trans. Electron Devices* **2010**, *57*, 3370; c) C. Jang, K. Kim, K. C. Choi, *J. Display Technol.* **2012**, *8*, 250.

[5] a) E. Downing, L. Hesselink, J. Ralston, R. Macfarlane, *Science* **1996**, *273*1185; b) T. Miteva, V. Yakutkin, G. Nelles, S. Baluschev, *New J. Phys.* **2008**, *10*, 103002; c) F. Wang, Y. Han, C. S. Lim, Y. Lu, J. Wang, J. Xu, H. Chen, C. Zhang, M. Hong, X. Liu, *Nature* **2010**, *463*, 1061.

[6] a) H. Ma, A. K. Y. Jen, L. R. Dalton, *Adv. Mater.* **2002**, *14*, 1339; b) W. H. Wong, E. Y. B. Pun, K. S. Chan, *Appl. Phys. Lett.* **2004**, *84*, 176.

[7] a) D. Matsuura, *Appl. Phys. Lett.* **2002**, *81*, 4526; b) T. J. Mullen, M. Zhang, W. Feng, R. J. El-khouri, L. Sun, C. Yan, T. E. Patten, G. Liu, *ACS Nano* **2011**, *5*, 6539; c) F. Zhang, Y. Deng, Y. Shi, R. Zhang, D. Zhao, *J. Mater. Chem.* **2010**, *20*, 3895.

[8] a) T. Konishi, M. Yamada, K. Soga, D. Matsuura, Y. Nagasaki, *J. Photopolym. Sci. Technol.* **2006**, *19*, 145; b) N. Venkatachalam, Y. Saito, K. Soga, *J. Am. Ceram. Soc.* **2009**, *92*, 1006; c) S. V. Eliseeva, J. G. Bünzli, *Chem. Soc. Rev.* **2010**, *39*, 189.

[9] a) A. Shalav, B. S. Richards, T. Trupke, K. W. Kramer, H. U. Gudel, *Appl. Phys. Lett.* **2005**, *86*, 013505; b) C. Strumpel, M. McCann, G. Beaucarne, V. Arkhipov, A. Slaoui, V. Svrcek, C. del Canizo, I. Tobias, *Sol. Energy Mater. Sol. Cells* **2007**, *91*, 238; c) G. B. Shan, G. P. Demopoulos, *Adv. Mater.* **2010**, *22*, 4373.

[10] Y. W. Jin, J. E. Jang, W. K. Yi, J. E. Jung, N. S. Lee, J. M. Kim, D. Y. Jun, J. P. Hong, *J. Vac. Sci. Technol., B* **1999**, *17*, 489.

[11] J. E. Jang, J. H. Gwak, Y. W. Jin, S. J. Lee, H. Park, J. E. Jung, N. S. Lee, *J. Vac. Sci. Technol. B* **2000**, *18*, 1106.

[12] a) M. Yu, J. Lin, Z. Wang, J. Fu, S. Wang, H. J. Zhang, Y. C. Han, *Chem. Mater.* **2002**, *14*, 2224; b) M. Yu, J. Lin, J. Fu, H. J. Zhang, Y. C. Han, *J. Mater. Chem.* **2003**, *13*, 1413; c) W. Wang, Z. Cheng, P. Yang, Z. Hou, C. Li, G. Li, Y. Dai, J. Lin, *Adv. Funct. Mater.* **2011**, *21*, 456.

[13] H. Si, D. Yuan, J. Chen, G. Chow, H. Zhang, *J. Colloid Interface Sci.* **2011**, *353*, 569.

[14] a) S. Watanabe, H. Hyodo, H. Taguchi, K. Soga, Y. Takanashi, M. Matsumoto, *Adv. Funct. Mater.* **2011**, *21*, 4264; b) S. Watanabe, H. Hyodo, H. Taguchi, K. Soga, Y. Takanashi, M. Matsumoto, *J. Oleo Sci.* **2012**, *61*, 565.

[15] S. Watanabe, T. Asanuma, H. Hyodo, K. Soga, M. Matsumoto, *Langmuir* **2013**, *29*, 11185.

[16] S. Watanabe, H. Shibata, S. Horiuchi, R. Azumi, H. Sakai, M. Abe, M. Matsumoto, *J. Colloid Interface Sci.* **2010**, *343*, 324.

[17] a) D. R. Gamelin, H. U. Güdel, *Top. Curr. Chem.* **2001**, *214*, 1; b) F. Auzel, *Chem. Rev.* **2004**, *104*, 139.

[18] J. Endo, J. Chen, D. Kobayashi, Y. Wada, H. Fujita, *Appl Opt.* **2002**, *41*, 1308.

[19] F. Wang, F. Wang, D. K. Chatterjee, Z. Li, Y. Zhang, X. Fan, M. Wang, *Nanotechnology* **2006**, *17*, 5786.